Lattice Boltzmann method modeling of magnetic water-based nanofluid through a permeable three-dimensional enclosure

M. Sheikholeslami[a,b], S.A. Shehzad[c,*], Ahmad Shafee[d], F.M. Abbasi[e] R. Kandasamy[f], and Zhixiong Lii[g,h]

[a]Department of Mechanical Engineering, Babol Noshirvani University of Technology, Babol, IRAN.
[b]Renewable energy systems and nanofluid applications in heat transfer Laboratory,
Babol Noshirvani, University of Technology, Babol, Iran.
[c]Department of Mathematics, COMSATS Institute of Information Technology, Sahiwal 57000, Pakistan.
*e-mail: ali_qau70@yahoo.com
[d]Public Authority of Applied Education and Training, College of Technological Studies,
Applied Science Department, Shuwaikh, Kuwait.
[e]Department of Mathematics, COMSATS Institute of Information Technology, Islamabad, Pakistan.
[f]FAST, University Tun Hussein Onn Malaysia, 86400, Parit Raja, Batu Pahat, Johor State, Malaysia.
[g]School of Engineering, Ocean University of China, Qingdao 266110, China.
[h]School of Mechanical, Materials, Mechatronic and Biomedical Engineering,
University of Wollongong, Wollongong, NSW 2522, Australia.

In this work, the mesoscopic theory is invoked to depict nanoparticle transportation through a porous cavity. Different amounts of Lorentz forces, Rayleigh number and permeability on the working fluid treatment have been examined. Al_2O_3-H_2O is selected including the Brownian motion effect. Isokinetic, streamlines, and isotherms contours are various shapes of outputs. Results illustrate that the increase in magnetic forces lead toan increase in the conduction mode. Dispersing nanoparticles aids to incrase the Hartmann number.

Keywords: Non-Darcy model; nanoparticle; lattice Boltzmann method; MHD; permeable space.

1. Introduction

Convection flow process has fascinated researchers due to its frequent uses fields such as electronic component cooling, food processing and crystal growth. Nanotechnology has been selected as a helpful passive methods to augment the rate of heating when magnetic forces exist. Haq *et al*. [1] scrutinized mass transfer of cross flow in a duct. They presented stream wise patterns in their report. Nawaz and Zubair [2] demonstrated the Hall Effect due to magnetic induction on radiative heat transfer of nano-plasma. They simulated in 3-dimensional spaces via FEM. Qi *et al*. [3] examined the application of TiO2 nanoparticles for cooling of Central Processing Unit (CPU). They scrutinized impacts of spherical bulges on the behavior of nanoparticles. Sheikholeslami *et al*. [4] illustrated the magnetizable hybrid nanofluid motion through a circular enclosure. They employed a variable magnetic force on the domain. Nabil *et al*. [5] demonstrated the peristaltic MHD flow of nanoparticles inside a duct. They considered various boundary conditions. Soomro *et al*. [6] scrutinized cooper nanoparticles transportation inside a cylinder. They reported a dual solution for the behavior of water based nanofluid. Sheikholeslami and Shehzad [7] scrutinized the nanoparticle flow through a permeable space due to MHD impact. Daniel *et al*. [8] considered the magnetic dissipation effect on stratification of nanofluid. They employed the radiation effect and viscous dissipation in energy equations. Hassan *et al*. [9] demonstrated Casson fluid transportation through a permeable media due to an external filed consid-

ering pulsatile flow. Rehman *et al*. [10] examined the nano liquid stagnation-point flow under magnetic field. They studied the exponential stretching sheet. Sheikholeslami [11] inspected the new way for simulation of nanoparticle exergy analysis under the Lorentz forces. Shoib *et al*. [12] examined the oscillating flow of non-Newtonian fluid over a plate. This plate was under the influence of MHD. Lu *et al*. [13] established the radiation effect on Carreau fluid behavior along a sheet. They added MHD impact with special boundary condition. Gibanov *et al*. [14] illustrated the second law behavior of nanoparticles in a cavity with a moving wall. They modeled mixed convection with a heat source. Astanina *et al*. [15] scrutinized natural convection of ferrofluid in an open porous cavity. Recent decade, different means have been employed to enhance the thermal properties of common fluid [16-43].

In this research, the effects of magnetic forces on migration of a water based nanofluid are displayed including the Darcy number impact. The 3D-problem is modeled by LBM. Outputs for various amounts of buoyancy, Darcy and Hartmann numbers are demonstrated.

2. Current geometry

A three-dimensional porous space filled with alumina is depicted in Fig. 1. The lower surface is hot and other boundaries are clear form that figure. A constant magnetic field is applied in the y direction.
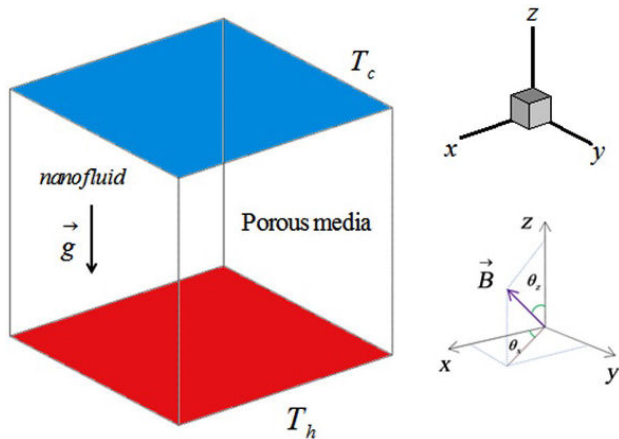
FIGURE 1. Current 3D enclosure.

3. Boltzmann equations and mesoscopic scheme

3.1. Boltzmann equations

Here we present an application of LBM. To estimate the velocity and temperature, we should solve Boltzmann equations whose unknowns are the two distribution functions (g and f). According to Ref. [44], we used BGK model to simplify the equations as follows

$$[-f_i(x,t) + f_i^{eq}(x,t)]\tau_v^{-1}\Delta t = f_i(x + \Delta t c_i, t + \Delta t)$$
$$- \Delta t c_i F_k - f_i(x,t), \tag{1}$$

$$\tau_C^{-1}[g_i^{eq}(x,t) - g_i(x,t)]\Delta t = -g_i(x,t)$$
$$+ g_i(x, \Delta t c_i, t + \Delta t). \tag{2}$$

In Eqs. (1) and (2), τ_v and τ_c are relaxation times for velocity and temperature. "i" represents each direction and in current mode this varies from 0 to 18 because we used the D3Q19 model (Fig. 2). In such model, Eq. (2) can be used to show the lattice velocity of each direction:
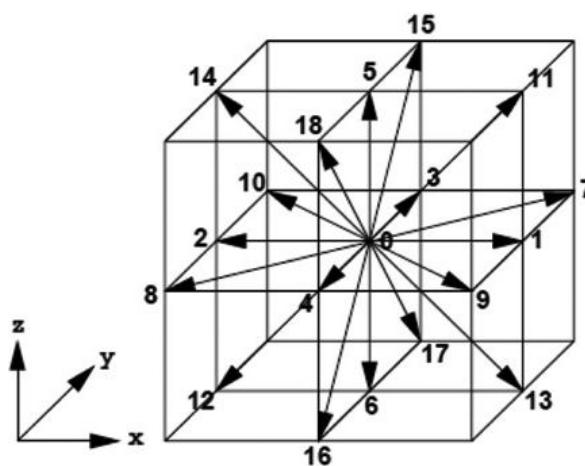

FIGURE 2. Selected model.

$$c_i = \begin{pmatrix} 0 & 0 & 0 & 0 & -1 & -1 & -1 & -1 & 1 & 1 & 1 & 0 & 0 & 0 & 0 & -1 & 1 & 0 \\ -1 & -1 & 1 & 1 & 0 & -1 & -1 & 1 & 0 & -1 & 1 & 0 & 0 & -1 & 1 & 0 & 0 & 0 \\ -1 & 1 & -1 & 1 & -1 & 0 & 0 & 0 & 1 & 0 & 0 & -1 & 1 & 0 & 0 & 0 & 0 & 0 \end{pmatrix} \tag{3}$$

We need to know the functions g_i^{eq} and f_i^{eq} which are given in [44]

$$w_i\left[1 + \frac{u \cdot C_i}{c_s^2}\right]T = g_i^{eq} \tag{4}$$

$$f_i^{eq} = \rho w_i\left[\frac{1}{2}\frac{(c_i \cdot u)^2}{c_s^4} - c_s^{-2}\frac{u^2}{2} + 1 + \frac{(u \cdot c_i)^2}{c_s^2}\right] \tag{5}$$

$$w_i = \{1/18 \ i = 1:6; \ 1/3 \ i = 0; 1/36 \ i = 7:18\} \tag{6}$$

External Lorentz and buoyancy forces act according to

$$F = F_z + F_y + F_x \tag{7}$$

$$F_z = 3\rho w_i\left[A\left(\sin(2\theta_z)\frac{v}{2} - \sin(\theta_x)\sin^2(\theta_z)w\right)\sin(\theta_x)\right.$$
$$\times (0.5\cos(2\theta_z)(u) - w\cos(\theta_x)\sin^2(\theta_z)$$
$$\left. + g_z\beta(T - T_m))A\cos(\theta_x)\right] - w(BB)(3)\rho w_i,$$

$$F_y = -3BBw_i\rho v + 3Aw_i\rho[-(v\cos^2(\theta_z)$$
$$- \sin(\theta_x)(0.5)w\sin(2\theta_z)) + (0.5u\sin(2\theta_x)\sin^2(\theta_z)$$
$$- v\sin^2(\theta_z)\cos^2(\theta_z x))],$$

$$F_x = -w_iBB(3)\rho u - 3\rho w_iA(-u\cos^2(\theta_z)$$
$$+ \sin(2\theta_z)w\cos(\theta_x)(0.5)) + 3w_iA(\sin^2(\theta_z)u\sin(\theta_x)$$
$$- v\cos(\theta_x)\sin^2(\theta_z))(-\sin(\theta_x)),$$

$$A = \mu L^{-2} Ha^2, \quad Ha = LB_0 \sqrt{\frac{\sigma}{\mu}},$$

$$Da = \frac{K}{L^2}, \quad BB = \frac{\upsilon}{DaL^2}.$$

where B_0 is magnitude of the magnetic field.

After solving the main equations, density, temperature and velocity can be calculated.

$$\text{Temperature:} \quad T = \sum_i g_i,$$

$$\text{Momentum:} \quad \rho u = \sum_i c_i f_i, \tag{8}$$

$$\text{Flow density:} \quad \rho = \sum_i f_i.$$

3.2. Characteristics of working liquid

The properties of the nanofluid selected as working fluid of current paper can be calculated as [45]

$$1 - \phi + \frac{(\rho C_p)_s}{(\rho C_p)_f \phi} = (\rho C_p)_{nf} / (\rho C_p)_f, \tag{9}$$

$$(\rho \beta)_{nf} = (\rho \beta)_f (1 - \phi) + \phi (\rho \beta)_s$$

$$\frac{\rho_{nf}}{\rho_f} = 1 + \frac{\rho_s}{\rho_f} \phi - \phi, \tag{10}$$

$$\Delta = \frac{\sigma_s}{\sigma_f},$$

$$1 + \left(\frac{-\phi(\Delta - 1) + (\Delta + 2)}{3\phi(\Delta - 1)} \right)^{-1} = \frac{\sigma_{nf}}{\sigma_f} \tag{11}$$

$$\chi = \frac{k_p}{k_f}, \quad R_f = -d_p(1/k_p - 1k_{p,eff}),$$

$$\frac{k_{nf}}{k_f} = 1 + 5 \times 10^4 \phi \rho_f c_{p,f} g'(\phi, T, d_p)$$

$$\times \sqrt{\frac{k_b T}{d_p \rho_p}} + \frac{3(\chi - 1)\phi}{(\chi + 2) - (\chi - 1)\phi} \tag{12}$$

$$g'(\phi, d_p, T) = (a_{10} Ln(d_p)^2 + a_7 Ln(d_p) + a_8 Ln(\phi)$$

$$+ a_6 Ln(d_p) + a_9 Ln(\phi)) + Ln(T)(a_1$$

$$+ a_3 Ln(\phi) + a_2 Ln(d_p) + a_4 Ln(d_p) Ln(\phi)$$

$$+ a_5 Ln(d_p)^2)$$

$$\mu_{nf} = k_f^{-1} \frac{\mu_f}{Pr} k_{\text{Brownian}} + (1 - \phi)^{-2.5} \mu_f \tag{13}$$

"nf", "s" and "f" represent "nanofluid", "solid particle" and "base fluid". "d_p" is the particle diameter.

We calculated three important variables namely, Kinetic energy, Nu_{ave} and Nu_{loc} according to below formulas:

$$E_c = 0.5[v^2 + w^2 + u^2]. \tag{14}$$

$$Nu_{ave} = \int_0^1 \int_0^1 Nu\, dY\, dX,$$

$$Nu_{loc} = \frac{k_{nf}}{k_f} \frac{\partial T}{\partial Z}\bigg|_{z=0}. \tag{15}$$

The required constraints are listed in Tables I and II.

TABLE I. Details for water and nanoparticles.

	ρ(kg/m³)	C_p(j/kgk)	k(W/mk)	d_p(nm)	$\sigma(\Omega \cdot \text{m})^{-1}$
Pure water	997.1	4179	0.613	-	0.05
Al₂O₃	3970	765	25	47	10^{-12}

TABLE II. The coefficient values of Al₂O₃ nanofluid.

Coefficient values	Al₂O₃- Water	Coefficient values	Al₂O₃- Water
a_1	52.813488759	a_6	-298.19819084
a_2	6.115637295	a_7	-34.532716906
a_3	0.6955745084	a_8	-3.9225289283
a_4	4.17455552786E-02	a_9	-0.2354329626
a_5	0.176919300241	a_{10}	-0.999063481

4. Independency of grid and validation

We should find unique solution which which are independent of the size. For this purpose, various grids have been used. As an example, Table III was reported. The code's validation is visualized in Fig. 3 and Table IV [46-48]).
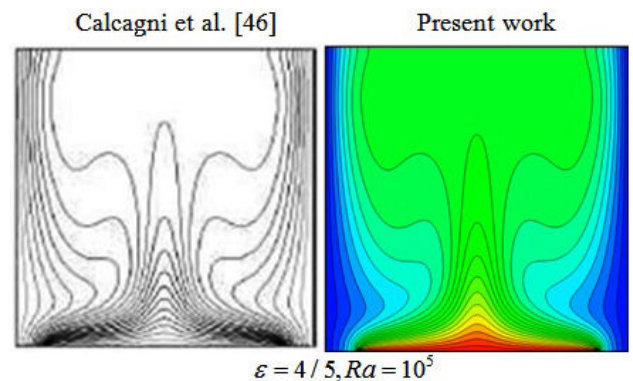

$$\varepsilon = 4/5, Ra = 10^5$$

FIGURE 3. Comparison of outputs between the present work and Ref. [46].

TABLE III. Grid independency when $Ra = 10^5$, $\phi = 0.04$ $Da = 100$ and $Ha = 60$.

Mesh size	$51 \times 51 \times 51$	$61 \times 61 \times 61$	$71 \times 71 \times 71$	$81 \times 81 \times 81$	$91 \times 91 \times 91$
Nu_{ave}	2.4167	2.4294	2.4371	2.4489	2.4499

TABLE IV. Nusselt number for various Ha at Pr=0.733.

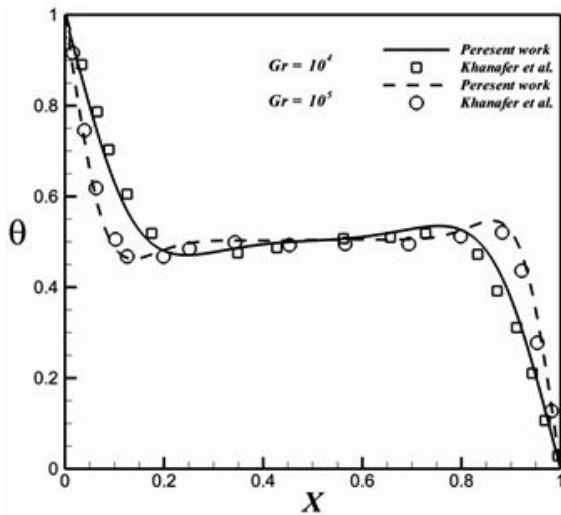| Ha	$Gr = 2 \times 10^4$	
	Present	Rudraiah *et al.* [48]
0	2.5665	2.566894
10	2.26626	2.261644
50	1.09954	1.083047
100	1.02218	1.008833

FIGURE 4. Validation of LBM code for nanofluid (Khanafer *et al.* [24]) when $\phi = 0.1$ and $Pr = 6.8$.

5. Results and discussion

In this report, we studied the behavior of a nanofluid in the presence of a uniform magnetic field inmersed in a 3D porous space. Using a homogenous model for the nanofluid, a nanoparticle concentration of 0.04 has been considered as working fluid. Outcomes are reported for various magnetic forces ($Ha = 60, 0$), buoyancy forces ($Ra = 10^5, 10^4$ and 10^3) and Darcy number ($Da = 100$, to 0.001).

Figures 5, 6, 7, 8, 9 and 10 illustrate the impact of the significant variables on the hydrothermal behavior. The domain is affected by conduction when buoyancy force and permeability are low. A simple shape for temperature contours can be observed. As these factors grow, convective mode is gradually increased. The complex shape of the temperature profile is a result of the convective mechanism. Stronger rotating vortex and thermal plumes can be seen for the largest Ra and Da. In this situation, that includes the effects of the

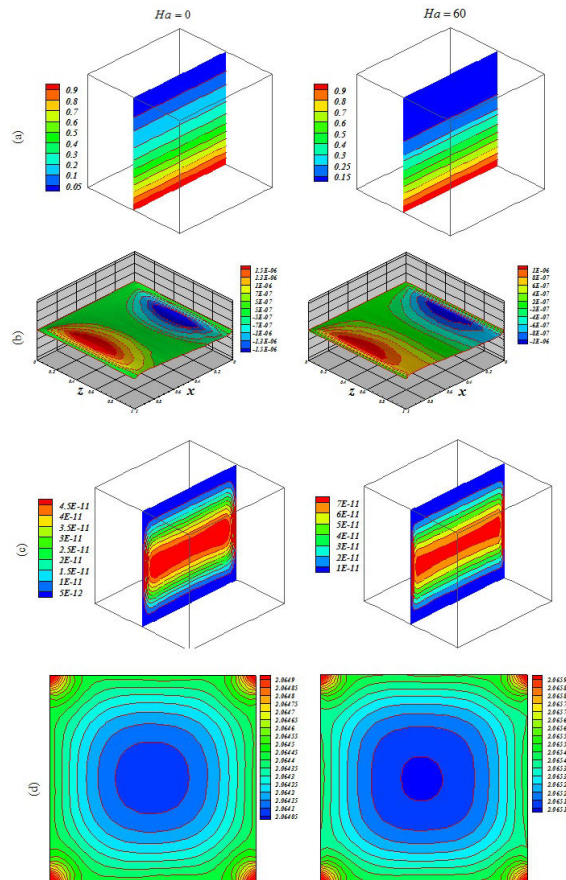magnetic field, the velocity is reduced and the

FIGURE 5. Influence of Lorentz forces on (a) isotherm, (b) streamlines, (c) isokinetic energy and (d) local Nusselt number at $Y = y/L = 0.5$ when $Ra = 10^3$, $Da = 0.001$, $\phi = 0.04$ $Ha = 0$ and $Ha = 60$.

convection to decrease. So, the kinetic energy is reduced with the increase of Ha. Besides, the thermal plume vanishes as a result of the of strong Lorentz forces. Fig. 11 demonstrates the variation of the heat transfer rate with respect to the variables. Equation (16) has been obtained according to the outcomes of various cases

$$Nu_{ave} = 2.22 + 0.58 \log(Ra) + 0.31Da - 0.29Ha$$
$$+ 0.46(\log(Ra))(Da) - 0.45(\log(Ra))(Ha)$$
$$- 0.32(Da)(Ha) + 0.56(\log(Ra))^2. \qquad (16)$$

The thickness of the boundary layer along the bottom surface decreases with the increase of Da and Ra. Nu decreases with the increase of Hartmann number. Increasing Ha makes the isotherms becomes denser.
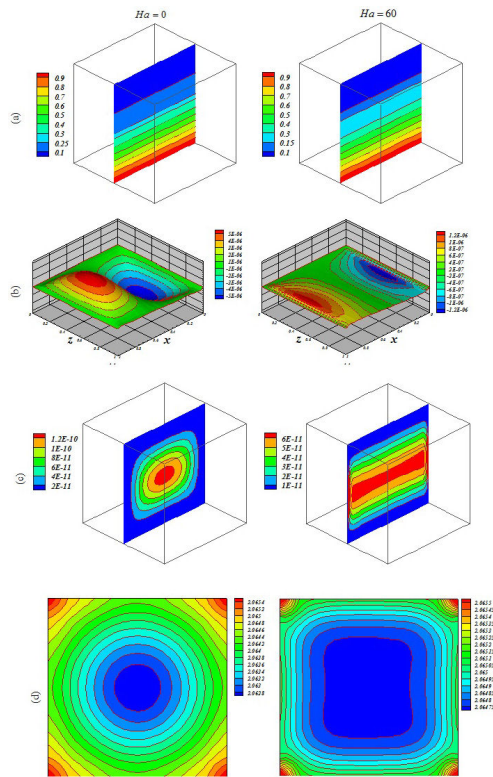
FIGURE 6. Influence of Lorentz forces on (a) isotherm, (b) streamlines, (c) isokinetic energy and (d) local Nusselt number at $Y = y/L = 0.5$ when $Ra = 10^3$, $Da = 100$, $\phi = 0.04$ $Ha = 0$ and $Ha = 60$.
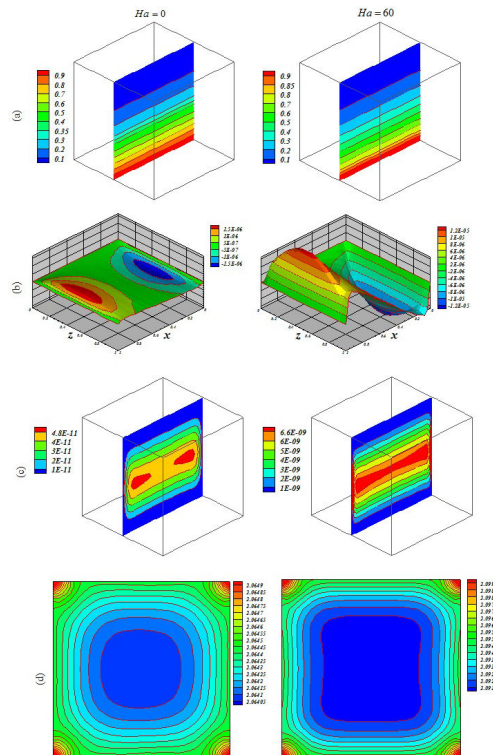

FIGURE 8. Influence of Lorentz forces on (a) isotherm, (b) streamlines, (c) isokinetic energy and (d) local Nusselt number at $Y = y/L = 0.5$ when $Ra = 10^4$, $Da = 100$, $\phi = 0.04$, $Ha = 0$ and $Ha = 60$.
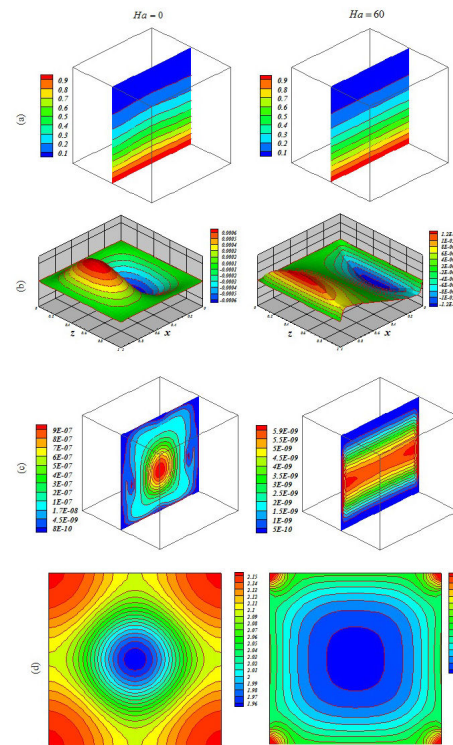

FIGURE 7. Influence of Lorentz forces on (a) isotherm, (b) streamlines, (c) isokinetic energy and (d) local Nusselt number at $Y = y/L = 0.5$ when $Ra = 10^4$, $Da = 0.001$, $\phi = 0.04$, $Ha = 0$ and $Ha = 60$.

FIGURE 9. Influence of Lorentz forces on (a) isotherm, (b) streamlines, (c) isokinetic energy and (d) local Nusselt number at $Y = y/L = 0.5$ when $Ra = 10^5$, $Da = 0.001$, $\phi = 0.04$, $Ha = 0$ and $Ha = 60$.
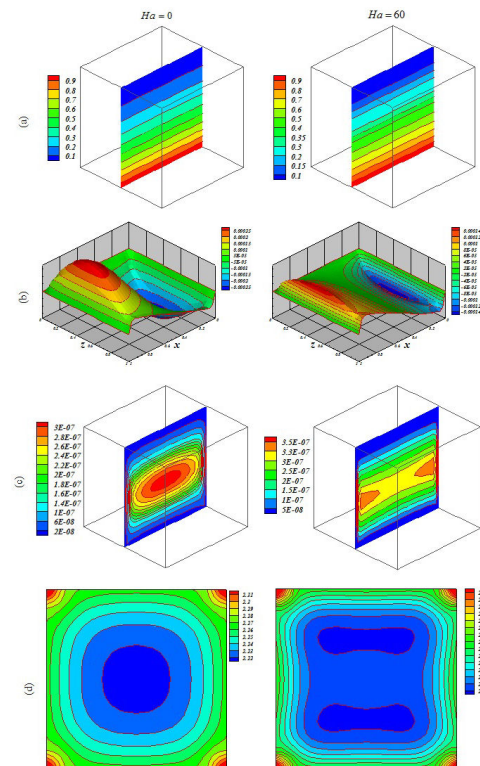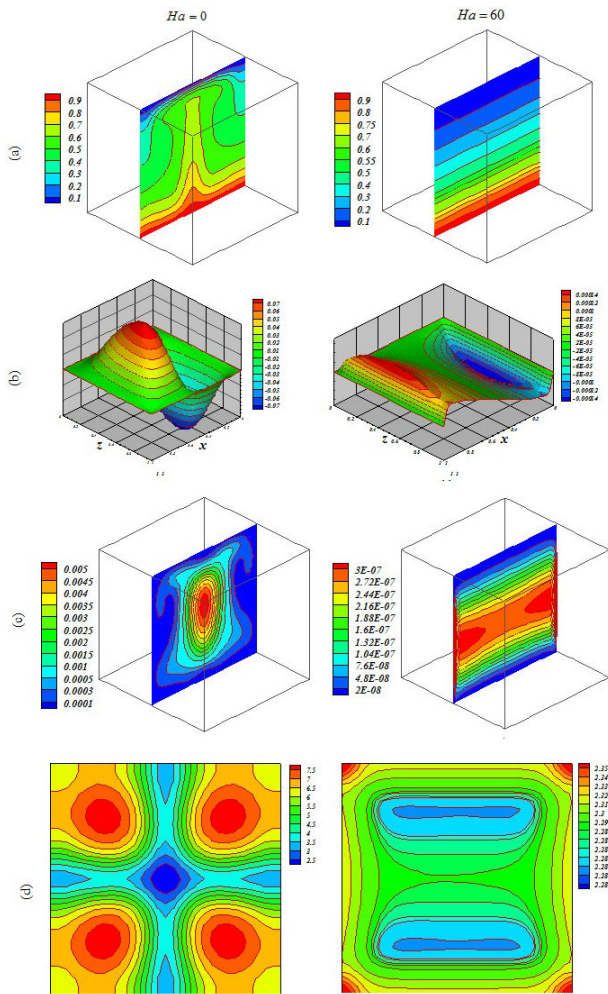
FIGURE 10. Influence of Lorentz forces on (a) isotherm, (b) streamlines, (c) isokinetic energy and (d) local Nusselt number at $Y = y/L = 0.5$ when $Ra = 10^5$, $Da = 100$, $\phi = 0.04$, $Ha = 0$ and $Ha = 60$.

FIGURE 11. Impacts of Da, Ra and Ha on average Nusselt number when $Ha = 30$, $Da = 50$ and $Ra = 10^4$.

6. Conclusions

In this mesoscopic modeling, the impact of a uniform Lorentz force on the convective transportat of nanoparticles through a porous 3D cavity has been studied. Lattice Boltzmann method which is founded on molecular theory can show ferrofluid behavior in no-Darcy medium. Such method provides the impact of Hartmann, Darcy numbers and buoyancy forces on ferrofluid. Results illustrated that the velocity of the nanofluid decreases with a decrease of buoyancy forces and permeability of space. As Lorentz forces enhance dispersing, nanoparticles becomes more significant. As permeability of space increases, the convective flow of nanofluid enhances.

Future work: As a new idea, this problem can be extended for variable magnetic field with hybrid nanofluid. Also, a two phase model for nanofluid can be employed.
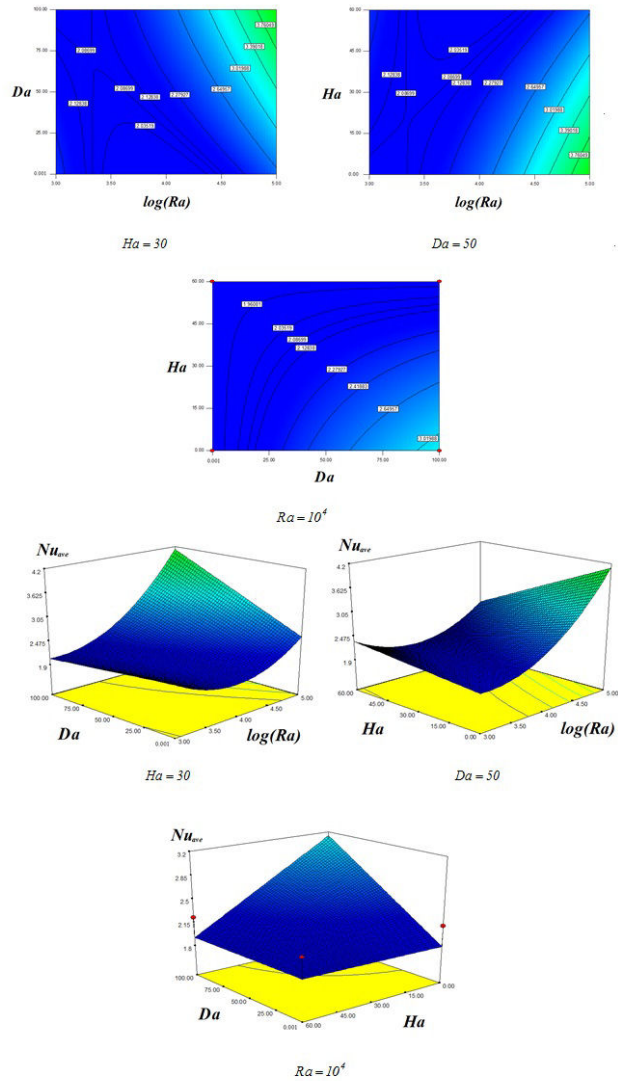
Nomenclature

Ha	Hartmann number
g, f	distribution functions
u, v, w	Velocity components
K	Permeability
Pr	Prandtl number
e_α	Discrete velocity
k	Thermal conductivity
c_s	Sound velocity
f^{eq}, g^{eq}	Equilibrium distribution
E_c	Kinetic energy
Greek symbols	
ψ	stream function

ρ	Fluid density
ϕ	Nanoparticles concentration
υ	Kinematic viscosity
σ	Electrical conductivity
τ	Lattice relaxation time
β	Thermal expansion coefficient
α	Thermal diffusivity

Subscripts

ave	Average
f	Pure fluid
loc	Local

Acknowledgments

1. R. Haq, F.A. Soomro, Z.H. Khan, and Q.M. Al-Mdallal, *Physical Journal Plus*, **132** (2017) 214.

2. M. Nawaz and T. Zubair, *Results in Physics* **7** (2017), 4111-4122.

3. C. Qi, N. Zhao, X. Cui, T. Chen, and J. Hu, *Int. J. Heat Mass Transf.* **123** (2018) 320-330.

4. M. Sheikholeslami, S.A.M. Mehryan, A. Shafee, and M.A. Sheremet, *Journal of Molecular Liquids*, **277** (2019) 388-396.

5. N.T.M. El-dabe, G.M. Moatimid, M.A. Hassan, and W.A. Godh, *Research International Journal*, **2** (2018) 00019.

6. F.A. Soomro, A. Zaib, R. Haq, and M. Sheikholeslami, *International Journal of Heat and Mass Transfer* **129** (2019) 1242-1249.

7. M. Sheikholeslami, and S.A. Shehzad, *International Journal of Heat and Mass Transfer* **106** (2017) 1261-1269.

8. Y.S. Daniel, Z.A. Aziz, Z. Ismail, and F. Salah, *Chinese Journal of Physics*, **55** (2017) 630-651.

9. M.A. Hassan, E.S.A. Nabil. T.M. El-dabe, and G.M. Moatimeid, *International Journal of Current Engineering and Technology, EISSN* 2277-4106, P-ISSN 2347-5161.

10. F. Ur Rehman, S. Nadeem, H. Ur Rehman, and R. Ul Haq, *Results in Physics* (2018) 8.

11. M. Sheikholeslami, *Computer Methods in Applied Mechanics and Engineering* **344** (2019) 319-333.

12. H. Shoib, T. Gul, S. Nasir, S. Islam, W. Ullah, and Z. Shah, *Journal of Applied Environmental and Biological Sciences*. **5** (2015) 25-34.

13. D. Lu, M. Ramzan, N. Huda, J.D. Chung, and U. Farooq, *Scientific Reports*, **8** (2018) 3709.

14. N.S. Gibanov, M.A. Sheremet, H.F. Oztop, and N. Abu-Hamdeh, *European Journal of Mechanics B/Fluids* **70** (2018) 148-159.

15. M.S. Astanina, M.A. Sheremet, H.F. Oztop, and N. Abu-Hamdeh, *International Journal of Mechanical Sciences* **136** (2018) 493-502.

16. M. Sheikholeslami, and S.A. Shehzad, *International Journal of Heat and Mass Transfer* **122** (2018) 1264-1271.

17. M. Sheikholeslami, and S.A. Shehzad, *International Journal of Heat and Mass Transfer* **120** (2018) 1200-1212.

18. K.R. Sekhar, G.V. Reddy, C.S.K. Raju, B. Pullepu, R. Kumar, and S.A. Shehzad, *International Journal of Nanoparticles* **9** (2017) 213-233.

19. Y. Qin, J. Luo, Z. Chen, G. Mei, L.-E. Yan, *Solar Energy* **171** (2018) 971-976.

20. M. Sheikholeslami, and S.A. Shehzad, *International Journal of Heat and Mass Transfer* **118** (2018) 182-192.

21. M. Sheikholeslami, and S.A. Shehzad, *International Journal of Heat and Mass Transfer* **115** (2017) 180-191.

22. W. Gao, L. Yan, L. Shi, *Optoelectronics and Advanced Materials-Rapid Communications*, **11** (2017) 119-124.

23. M. Sheikholeslami, S.A. Shehzad, F.M. Abbasi, and Li Zhixiong, *Computer Methods in Applied Mechanics and Engineering* **338** (2018) 491-505.

24. M. Sheikholeslami, M. Jafaryar, and Li Zhixiong, *International Journal of Heat and Mass Transfer* **124** (2018) 980-989.

25. Y. Qin, *Renewable and Sustainable Energy Reviews*, **52** (2015) 445-459

26. W. Gao, W. F. Wang, *Chaos, Solitons and Fractals*, **89** (2016) 290-294.

27. M. Sheikholeslami, and S.A. Shehzad, *International Journal of Heat and Mass Transfer* **113** (2017) 796-805.

28. H. Hammed, M. Haneef, Z. Shah, S. Islam, W. Khan, and S. Muhammad, *Appl. Sci.* **8** (2018) 160. doi:10.3390/app8020160.

29. M. Sheikholeslami, S.A. Shehzad, and Li. Zhixiong, *International Journal of Heat and Mass Transfer* **125** (2018) 375-386.

30. M. Sheikholeslami, *Computer Methods in Applied Mechanics and Engineering* **344** (2019) 306-318.

31. Y. Qin, Y. He, J.E. Hiller, G. Mei, Journal of Cleaner Production **199** (2018) 948-956

32. M. Sheikholeslami, R. Haq, A. Shafee, and Z. Li, *International Journal of Heat and Mass Transfer* **130** (2019) 1322-1342.

33. W. Gao, W. F. Wang, *International Journal of Computer Mathematics*, **95** (2018) 1527-1547.

34. M. Sheikholeslami, M. Jafaryar, A. Shafee, and Z. Li, *Journal of Thermal Analysis and Calorimetry*, (2019). DOI: 10.1007/s10973-018-7866-7

35. H. Sajjadi, and G.H.R. Kefayati, *Heat Transfer-Asian Research* **45** (2016) 795- 814.

36. W. Gao, M. R. Farahani, *The Computer Journal* **60** (2017) 1289-1299.

37. M. Sheikholeslami, M. Barzegar Gerdroodbary, R. Moradi, Ahmad Shafee, and Zhixiong Li, *Computer Methods in Applied Mechanics and Engineering*, **344** (2019) 1-12.

38.] M. Sheikholeslami, *Journal of Molecular Liquids* **266** (2018) 495-503.

39. M. Sheikholeslami, *Journal of Molecular Liquids* **265** (2018) 347-355.

40. Sun Fengrui, Yao Yuedong, and Li Xiangfang, *The Heat and Mass Transfer Characteristics of Superheated Steam Coupled with Non-condensing Gases in Horizontal Wells with Multi-point Injection Technique. Energy,* (2018) **143** 995-1005.

41. Y. Qin, Y. Zhao, X. Chen, L. Wang, F. Li, and T. Bao, *Construction and Building Materials* **215** (2019) 114-118.

42. G. C. Dash, R. S. Tripathy, M. M. Rashidi, and S. R. Mishra, *Journal of Molecular Liquids* **221** (2016) 860-866.

43. W. Gao, L. Liang, T. W. Xu, and J. H. Gan, *Open Physics*, **15** (2017) 501-508.

44. Y.Y. Yan, and Y.Q. Zu, *Int. J. Heat Mass Transfer* **51** (2008) 2519-2536.

45. M.S. Kandelousi, *Phys. Lett. A* **378** (2014) 3331-3339.

46. B. Calcagni, F. Marsili, and M. Paroncini, *Appl. Thermal Eng.* **25** (2005) 2522-2531.

47. K. Khanafer, K. Vafai, and M. Lightstone, *Int. J. Heat Mass Transfer* **46** (2003) 3639-3653.

48. N. Rudraiah, R.M. Barron, M. Venkatachalappa, and C.K. Subbaraya, *Int. J. Eng. Sci.* **33** (1995) 1075-1084.